

This work has been submitted to IFAC for possible publication
Submitted to 10th Vienna International Conference on Mathematical
Modelling

Mathematical Modeling for Holistic Convex Optimization of Hybrid Trains

Rabee Jibrin, Stuart Hillmansen, Clive Roberts

*Department of Electronic, Electrical and Systems Engineering,
University of Birmingham, Birmingham, United Kingdom
e-mail: rxj956 , s.hillmansen , c.roberts.20 @bham.ac.uk*

Abstract: We look into modeling fuel cell hybrid trains for the purpose of optimizing their operation using convex optimization. Models and constraints necessary to form a physically feasible yet convex problem are reviewed. This effort is described as holistic due to the broad consideration of train speed, energy management system, and battery thermals. The minimized objective is hydrogen fuel consumption for a given target journey time. A novel battery thermal model is proposed to aid with battery thermal management and thus preserve battery lifetime. All models are derived in the space-domain which along constraint relaxations guarantee a convex optimization problem. First-principle knowledge and real-world data justify the suitability of the proposed models for the intended optimization problem.

Keywords: Railways, Hybrid Vehicles, Dynamic Modelling, Convex Optimisation, Energy Management Systems.

1. INTRODUCTION

1.1 Motivation

Hydrogen fuel cell hybrid trains are expected to play a key role in decarbonizing the railways owing to their lack of harmful emissions at point-of-use and adequate driving range; however, their total cost of ownership is projected to be higher than incumbent diesel trains primarily due to the higher cost of hydrogen fuel in comparison to diesel fuel (Pagenkopf and Kaimer, 2014). We aim at reducing hydrogen fuel consumption by optimizing train operation. Models for a convex optimization problem are sought after in order to alleviate computational concerns.

1.2 Background

Train speed optimization has been researched extensively owing to the large contribution of traction power towards rail energy consumption (Scheepmaker et al., 2017). More recently, Lhomme et al. (2018) brought attention to the energy management system (EMS) of fuel cell hybrid trains by holding the 2019 IEEE VTS Motor Vehicles Challenge. The EMS determines power distribution among a hybrid vehicle's power-sources and is thus a vital determinant of efficiency. Yue et al. (2019) reviewed an extensive body of literature for fuel cell hybrid EMS. Simulation results by García et al. (2013) suggest that optimization-based algorithms outperform their rule-based counterparts which motivates our current focus on the former.

While the aforementioned address either speed or EMS separately, some works have attempted to optimize both within a single optimization problem (concurrently) in order to achieve better solution optimality by embedding knowledge of the dynamic coupling between both trajectories, e.g., dynamic programming (Xiao et al., 2021), indi-

rect optimal control (Chen et al., 2019), integer programming (Wu et al., 2021), and relaxed convex optimisation (Ebbesen et al., 2018; Jibrin et al., unpublished).

The high capital cost of traction batteries has also motivated many to consider penalizing (Moura et al., 2013) or bounding (Ebbesen et al., 2012) battery degradation, though strictly within the EMS problem setting—speed is optimized beforehand separately. The semi-empirical battery degradation model presented by Wang et al. (2011) as a function of temperature, state-of-charge, and C-rate, is the most often used. A common assumption among optimization-based algorithms that consider battery degradation is an active cooling system that maintains a constant battery temperature which simplifies the degradation model to static temperature. This simplification can lead to unexpected battery degradation when subject to non-ideal thermal management in the real-world (Filippi et al., 2010). Therefore, dropping the static temperature assumption could further benefit battery lifetime, especially in light of experimental results that designate elevated temperatures as the leading cause of battery degradation (Lucu et al., 2020). Moreover, including thermal constraints during speed planning can limit the reliance on the active cooling system and thus reduce its parasitic energy draw (Park and Ahn, 2021). Algorithms that did consider battery temperature as a bounded dynamic state have done so strictly within the EMS problem setting and often at great computational cost, e.g., genetic algorithm (Li et al., 2019), dynamic programming (Tang, 2017), and relaxed convex optimization (Kim et al., 2020).

1.3 Contribution and Outline

Literature lacks a method to concurrently optimize hybrid vehicle speed and EMS while considering battery thermal constraints. The high predictability of railway environ-

ments promises substantial returns for such an elaborate and holistic optimization approach. This paper gathers the models necessary to form a convex optimization problem for the aforementioned goal. Furthermore, a novel thermal model for the battery is proposed. Future publications will showcase these models within a realistic optimization case study, though preliminary results by the authors can be found in (Jibrin et al., unpublished).

Section 2 introduces the train's longitudinal dynamics, section 3 covers the powertrain's models, and section 4 uses these models to formulate the optimization problem.

2. LONGITUDINAL DYNAMICS

2.1 Choice of Modeling Domain

Common among model-based optimization for dynamic systems is to model the system in the time-domain, i.e., the model predicts system state after a temporal interval of Δ_t seconds. However, a complication from optimizing vehicle speed in the time-domain is interpolating track information, e.g., gradient, when the physical location for a given temporal interval is dependent on the optimized speed and thus unknown *a priori*. This can be addressed by relying on historical speed data to predict location against time however significant location errors could accumulate over a long journey. Alternatively, more sophisticated methods such as the pseudospectral method can be used at a great computational cost (Scheepmaker et al., 2017).

Instead of the often used time-domain, the current problem setting lends itself more readily to the space-domain, i.e., the model predicts system state after a spatial interval of Δ_s meters longitudinally along the track. As such, one can accurately retrieve track information for any interval by directly referring to its respective location in space. Herein, we formulate the models in the discrete space-domain with zero-order hold between intervals. The entire journey's longitudinal space is divided into a grid of N intervals.

2.2 Train Longitudinal Speed

Douglas et al. (2016) assume the train as a point mass m with an equivalent inertial mass m_{eq} . The train's longitudinal speed v is influenced by traction motor force F_m , mechanical brakes force F_{brk} , and the external forces acting on the train F_{ext} which is the summation of the Davis Equation $a + bv_i + cv_i^2$ and gravitational pull $mg \sin(\theta_i)$. To predict speed after a single spatial interval, construct

$$\frac{1}{2}m_{eq}v_{i+1}^2 = \frac{1}{2}m_{eq}v_i^2 + (F_{m,i} + F_{brk,i})\Delta_{s,i} - F_{ext,i}\Delta_{s,i} \quad (1)$$

using the definition of kinetic energy $E_{k.e.} = 1/2m_{eq}v^2$, the definition of mechanical work $E_{work} = F\Delta_s$, and the principle of energy conservation. Equation (1) is nonlinear in v but can be linearized by substituting the quadratic terms v^2 with z and keeping the non-quadratic terms v unchanged, namely

$$\frac{1}{2}m_{eq}z_{i+1} = \frac{1}{2}m_{eq}z_i + (F_{m,i} + F_{brk,i})\Delta_{s,i} - F_{ext,i}\Delta_{s,i} \quad (2)$$

and

$$F_{ext,i} = a + bv_i + cz_i + mg \sin(\theta_i). \quad (3)$$

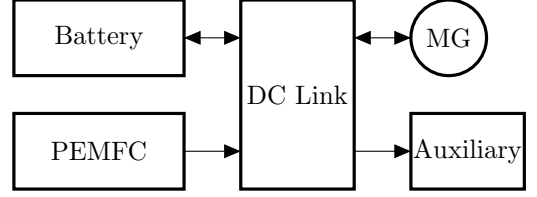


Fig. 1. Fuel cell series hybrid architecture. Arrows depict feasible directions of electric power flow.

The linear model (2) relies on both v and z to define train speed and thus requires the non-convex equality constraint $v^2 = z$ to hold true which is subsequently relaxed into the convex inequality

$$v^2 \leq z. \quad (4)$$

2.3 Journey Target Time

Total journey time is expressed as summation of time required for all intervals $\sum_{i=1}^N \Delta_s/v_i$ but is non-linear in v . This expression can be replaced by the linear

$$\sum_{i=1}^N \Delta_s \lambda_{v,i} \quad (5)$$

when used along the auxiliary non-convex equality $\lambda_v = 1/v$ which is then relaxed into the convex inequality

$$\lambda_v \geq 1/v \quad (6)$$

for $v, \lambda_v > 0$ (Boyd and Vandenberghe, 2004). Section 4 explains how the strict positivity constraints imposed on speed have a negligible impact on solution optimality and how the relaxed inequalities (4) and (6) hold with equality at the optimal solution.

3. POWERTRAIN MODELING

Figure 1 depicts the powertrain considered, a polymer electrolyte membrane fuel cell (PEMFC) in a series hybrid configuration with a lithium-ion battery. The components considered herein are the battery, fuel cell, motor-generator (MG), and vehicle auxiliary loads. The term motor is used interchangeably with motor-generator. The following subsections present the models and constraints for each component. Without loss of generality, repeated components are aggregated and modeled as a single bigger component, optimized as the newly formed single big component, after which the optimized solution is divided equally upon the actual individual instances of that component, e.g., the traction motors are modeled and optimized as a single big motor acting on the point mass.

3.1 Traction Motor

The electric power flow in Fig. 1 is described by

$$P_m/\eta_m(P_m) + P_{aux} = P_{fc} + P_{batt}, \quad (7)$$

where P_m is motor mechanical power, $\eta_m(P_m)$ is motor efficiency and thus $P_m/\eta_m(P_m)$ is electric power at motor terminals, P_{aux} is auxiliary load, P_{fc} is fuel cell electric power output, and P_{batt} is battery electric power output.

The power balance expression (7) requires the non-convex constraint $P_m = F_m v$ to hold true in order to use it in

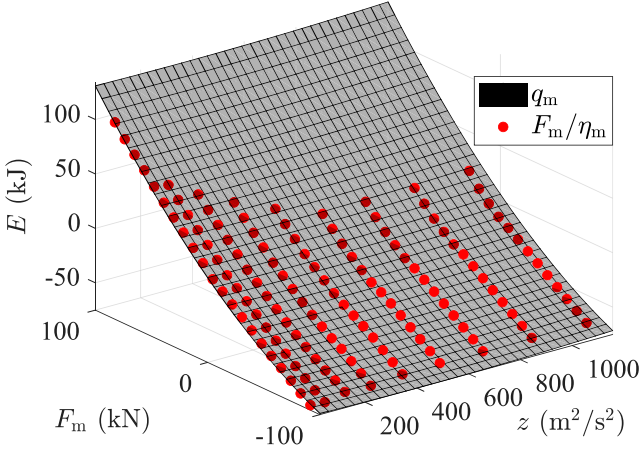


Fig. 2. Motor data from Wipke et al. (1999). $\Delta_s = 1$.

conjunction with the speed model (2). To resolve this non-convexity, start by dividing (7) by v to yield

$$F_m/\eta_m(F_m, z) + P_{\text{aux}}\lambda_v = F_{\text{fc}} + F_{\text{batt}}, \quad (8)$$

where motor efficiency is defined as $\eta_m(F_m, z)$ instead of $\eta_m(P_m)$, recall $P = F\sqrt{z}$. The alternative model (8) expresses energy flow per longitudinal meter traveled, recall $E_{\text{work}} = F\Delta_s$ and $F = P\lambda_v$. The forces F_{fc} and F_{batt} are fictitious but numerically represent each component's energy contribution. Since (8) is directly written in terms of F_m the non-convex equality constraint $P_m = F_mv$ is no longer necessary.

The equality (8) is non-convex due to the non-linearity in $F_m/\eta_m(F_m, z)$. Moreover, motor efficiency, η_m , is typically a discrete look-up table rather than a smooth function. Jia et al. (2020) accurately approximated $F_m/\eta_m(F_m, z)$ with the convex quadratic polynomial $q_m(F_m, z) := p_{00} + p_{10}z + p_{01}F_m + p_{11}F_mv + p_{20}z^2 + p_{02}F_m^2$, as shown in Fig. 2, which can be used to relax (8) into the convex inequality

$$q_m(F_m, z) + P_{\text{aux}}\lambda_v \leq F_{\text{fc}} + F_{\text{batt}}. \quad (9)$$

The convex polynomial $q_m(F_m, z)$ can be guaranteed to accurately approximate $F_m/\eta_m(F_m, z)$ for all motors known, as efficiency is practically concave in power (De Almeida et al., 2011) the reciprocal of which is convex (Boyd and Vandenberghe, 2004).

The remaining aspect to be covered is motor operational constraints. Motors operate within two regions depending on rotational velocity, a constant force region under the cutoff speed expressed by the simple bounds

$$\underline{F_m} \leq F_m \leq \overline{F_m} \quad (10)$$

and a constant power region above the cutoff speed expressed by the linear inequalities

$$\underline{P_m}\lambda_v \leq F_m, \quad (11a)$$

$$F_m \leq \overline{P_m}\lambda_v. \quad (11b)$$

3.2 Fuel Cell

To penalize hydrogen fuel consumption in the space-domain, we derive an expression for fuel energy consumed per longitudinal meter traveled. Using the look-up table efficiency model $\eta_{\text{fc}}(F_{\text{fc}}, z)$, the exact fuel penalty per meter is $F_{\text{fc}}/\eta_{\text{fc}}(F_{\text{fc}}, z)$. Thorstensen (2000) proved using first-principle models that all fuel cell technologies admit

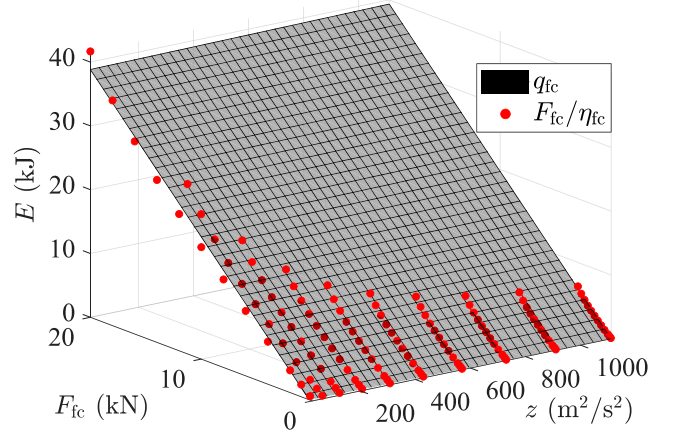


Fig. 3. Fuel cell data from Wipke et al. (1999). $\Delta_s = 1$.

a concave efficiency curve with power which implies that the exact penalty can be accurately approximated by the convex quadratic polynomial

$$q_{\text{fc}}(F_{\text{fc}}, z) := p'_{00} + p'_{10}z + p'_{01}F_{\text{fc}} + p'_{11}F_{\text{fc}}v + p'_{20}z^2 + p'_{02}F_{\text{fc}}^2, \quad (12)$$

as shown by Fig. 3.

The fuel cell power constraints are expressed by

$$\underline{P_{\text{fc}}}\lambda_v \leq F_{\text{fc}}, \quad (13a)$$

$$F_{\text{fc}} \leq \overline{P_{\text{fc}}}\lambda_v, \quad (13b)$$

where the lower bound $\underline{P_{\text{fc}}}$ could be selected as strictly positive in order to curtail the excessive degradation that accompanies idling and restarting.

3.3 Battery State-of-Charge

Predicting the battery's state-of-charge ζ is vital in order to guarantee charge-sustaining operation—terminal battery charge identical to initial. The battery is modeled with a fixed open-circuit voltage U_{oc} and a fixed internal resistance R , a model that is accurate for the narrow state-of-charge range employed by hybrid vehicles. Experimental results by Ghaviha et al. (2019) validate this model.

Pelletier et al. (2017) derive the change of state-of-charge

$$\Delta_{\zeta} = \frac{U_{\text{oc}} - \sqrt{U_{\text{oc}}^2 - 4P_{\text{batt}}R}}{2R} \cdot \frac{1}{3600Q} \cdot \Delta_t, \quad (14)$$

where Q is battery charge capacity, valid for $P_{\text{batt}} \leq U_{\text{oc}}^2/4R$. Accordingly, a positive/(negative) P_{batt} will discharge/(charge) the battery

$$\zeta_{i+1} = \zeta_i - \Delta_{\zeta, i}. \quad (15)$$

For a given Δ_t the model (14) is convex in P_{batt} because the negative sign preceding the concave square root flips it into a convex term. This empowers the convex quadratic polynomial $q_{\zeta}(P_{\text{batt}}) := \alpha P_{\text{batt}}^2 + \beta P_{\text{batt}}$ to accurately approximate (14), as shown by Fig. 4. Nevertheless, an expression written in terms of spatial intervals Δ_s rather than temporal Δ_t needs to be found to complete a space-domain formulation. To derive such, start by assuming $\Delta_{\zeta} = q_{\zeta}(P_{\text{batt}})\Delta_t$

$$\Delta_{\zeta} = (\alpha P_{\text{batt}}^2 + \beta P_{\text{batt}})\Delta_t \quad (16)$$

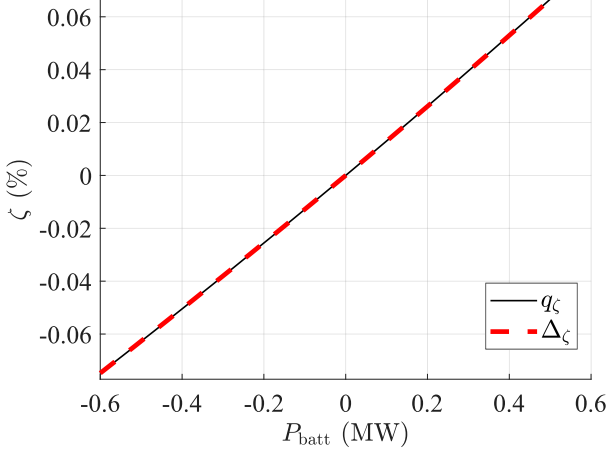


Fig. 4. Battery data from Stroe (2018). $\Delta_t = 1$.

which can be rewritten in terms of F_{batt} as

$$\Delta_\zeta = (\alpha F_{\text{batt}}^2 v^2 + \beta F_{\text{batt}} v) \Delta_t \quad (17)$$

followed by the substitution $v = \Delta_s / \Delta_t$

$$\Delta_\zeta = \left(\alpha F_{\text{batt}}^2 v \frac{\Delta_s}{\Delta_t} + \beta F_{\text{batt}} \frac{\Delta_s}{\Delta_t} \right) \Delta_t \quad (18)$$

then cancel out Δ_t in order to obtain the spatial expression

$$\Delta_\zeta = \alpha F_{\text{batt}}^2 v \Delta_s + \beta F_{\text{batt}} \Delta_s. \quad (19)$$

Equation (19) is non-convex but can be rewritten as

$$\alpha F_{\text{batt}}^2 \Delta_s = \frac{\Delta_\zeta - \beta F_{\text{batt}} \Delta_s}{v} \quad (20)$$

then subsumed into

$$\alpha F_{\text{batt}}^2 \Delta_s = \lambda_\zeta \lambda_v \quad (21)$$

using the linear auxiliary constraint

$$\lambda_\zeta = \Delta_\zeta - \beta F_{\text{batt}} \Delta_s \quad (22)$$

and the convex constraint (6).

The relaxation of the non-convex equality (21),

$$\alpha F_{\text{batt}}^2 \Delta_s \leq \lambda_\zeta \lambda_v, \quad (23)$$

forms a convex feasible set for $\lambda_\zeta, \lambda_v \geq 0$ which is nonrestrictive, since λ_v and the left-hand side of (23) are non-negative by definition.

3.4 Battery Temperature

Battery temperature T_{batt} is to be modeled in order to keep temperature under the upper bound

$$T_{\text{batt}} \leq \overline{T_{\text{batt}}} \quad (24)$$

in order to preserve battery health. For a change in temperature of ΔT_{batt} between intervals, battery temperature is predicted using the linear

$$T_{\text{batt},i+1} = T_{\text{batt},i} + \Delta T_{\text{batt},i}. \quad (25)$$

Changes in temperature are caused by the electrochemical losses during use, the heat lost passively to the surroundings, and the heat extracted by the active cooling system. Lin et al. (2021) model the battery as a lumped mass m_{batt} with thermal capacity c_{batt} that admits a thermal content change of $m_{\text{batt}} c_{\text{batt}} \Delta T_{\text{batt}}$ for a change ΔT_{batt} . Using the fictitious forces convention, the heat balance between spatial intervals is

$$m_{\text{batt}} c_{\text{batt}} \Delta T_{\text{batt}} = (F_{\text{gen}} - F_{\text{lost}}) \Delta_s, \quad (26)$$

where F_{gen} and F_{lost} denote the heat generated and lost per meter traveled, respectively.

Derivation of Heat Generated F_{gen} can be directly expressed in terms of battery efficiency for both charging and discharging as

$$F_{\text{gen}} = |F_{\text{batt}}| (1 - \eta_{\text{batt}}(F_{\text{batt}}, v)), \quad (27)$$

where

$$\eta_{\text{batt}}(F_{\text{batt}}, v) := \begin{cases} U_{\text{batt}}(F_{\text{batt}} v) / U_{\text{oc}} & F_{\text{batt}} \geq 0 \\ U_{\text{oc}} / U_{\text{batt}}(F_{\text{batt}} v) & \text{otherwise} \end{cases} \quad (28)$$

and

$$U_{\text{batt}}(P) := (U_{\text{oc}} + \sqrt{U_{\text{oc}}^2 - 4P_{\text{batt}} R}) / 2. \quad (29)$$

However, the equality (26) cannot maintain its linear status if it were to admit the absolute value operation $|F_{\text{batt}}|$ as required by (27). Alternatively, we propose to mimic $|F_{\text{batt}}|$ by $F_{\text{dis}} - F_{\text{chr}}$ as in

$$F_{\text{gen}} = (F_{\text{dis}} - F_{\text{chr}}) (1 - \eta_{\text{batt}}(F_{\text{batt}}, v)), \quad (30)$$

where $F_{\text{dis}} \geq F_{\text{batt}}, 0$ and $F_{\text{chr}} \leq F_{\text{batt}}, 0$. Section 4 explains how F_{dis} and F_{chr} adopt the positive discharging and negative charging values of F_{batt} , respectively. Lastly, the variable efficiency term $\eta_{\text{batt}}(F_{\text{batt}}, v)$ in (30) impedes a linear expression due to its multiplication by the variables F_{dis} and F_{chr} . Instead, we propose to simplify (30) using constant efficiency terms

$$F_{\text{gen}} = F_{\text{dis}} (1 - \eta_{\text{dis}}) - F_{\text{chr}} (1 - \eta_{\text{chr}}), \quad (31)$$

where η_{dis} and η_{chr} denote average discharging and charging efficiency, respectively.

Derivation of Heat Lost The heat lost per meter traveled

$$F_{\text{lost}} = F_{\text{amb}} + F_{\text{act}} \quad (32)$$

comprises losses to ambient F_{amb} and active cooling system F_{act} . The heat lost to ambient is easiest expressed as $h(T_{\text{batt}} - T_{\text{amb}}) \Delta_t$, where h is rate of heat transfer per second. Upon substituting $\Delta_t = 1/v$ into the aforementioned

$$F_{\text{amb}} = h(T_{\text{batt}} - T_{\text{amb}}) \lambda_v. \quad (33)$$

Compilation of Thermal Model Upon substituting and expanding (31) and (33) into (26) we get

$$\begin{aligned} m_{\text{batt}} c_{\text{batt}} \Delta T_{\text{batt}} = & (F_{\text{dis}} (1 - \eta_{\text{dis}}) - F_{\text{chr}} (1 - \eta_{\text{chr}}) \\ & - h T_{\text{batt}} \lambda_v + h T_{\text{amb}} \lambda_v \\ & - F_{\text{act}}) \Delta_s \end{aligned} \quad (34)$$

which is almost linear except for the term $h T_{\text{batt}} \lambda_v$. Replace this non-linear term by the relaxed inequality

$$\lambda_T \leq h T_{\text{batt}} \lambda_v \quad (35)$$

for $T_{\text{batt}}, \lambda_v \geq 0$ to get the entirely linear

$$\begin{aligned} m_{\text{batt}} c_{\text{batt}} \Delta T_{\text{batt}} = & (F_{\text{dis}} (1 - \eta_{\text{dis}}) - F_{\text{chr}} (1 - \eta_{\text{chr}}) \\ & - \lambda_T + h T_{\text{amb}} \lambda_v \\ & - F_{\text{act}}) \Delta_s. \end{aligned} \quad (36)$$

The non-negative condition imposed on T_{batt} is nonrestrictive, since a temperature of negative kelvin is physically infeasible. Section 4 explains how the inequality (35) holds with equality when the upper temperature bound (24) is approached.

4. OPTIMIZATION FORMULATION

The models derived in sections 2 and 3 are now used to formulate the target optimization problem. The optimized system states are $(z, \zeta, T_{\text{batt}})$; the main control variables are $(F_{\text{m}}, F_{\text{brk}}, F_{\text{fc}}, F_{\text{batt}}, F_{\text{act}})$; and the auxiliary variables are $(v, \lambda_v, \lambda_\zeta, \lambda_T, \Delta_\zeta, \Delta T_{\text{batt}}, F_{\text{pos}}, F_{\text{neg}})$. After obtaining the optimal trajectories to the fictitious force variables $(F_{\text{fc}}, F_{\text{batt}}, F_{\text{act}})$, they are to be multiplied by the velocity trajectory in order to obtain their respective commands in terms of power.

The optimization problem computes the trajectory for N intervals from $i = 0, 1, \dots, N-1$ starting with initial states $(z_0, \zeta_0, T_{\text{batt},0})$. The cost function

$$\sum_i \left(q_{\text{fc}}(F_{\text{fc},i}, z_i) + F_{\text{act},i} \right) \Delta_{\text{s},i} \quad (37)$$

penalizes hydrogen fuel consumption and the parasitic draw of the active cooling system.

The linear equality constraints (2), (15), and (25), predict the system's states $(z, \zeta, T_{\text{batt}})$, respectively. A second set of necessary linear equality constraints are (22) and (36) for the auxiliary variables λ_ζ and ΔT_{batt} . Moreover, the equality

$$\zeta_N = \zeta_0 \quad (38)$$

enforces charge-sustaining operation on the battery,

$$\sum_i \Delta_{\text{s},i} \lambda_{v,i} = \tau \quad (39)$$

terminates the journey exactly τ seconds after start, and

$$z_j = z_{\text{stop}} \quad (40)$$

halts the train at station stop intervals denoted j .

The linear inequality constraints are broken down into the simple lower and upper bounds

$$F_{\text{chr},i} \leq 0 \leq \lambda_{v,i}, \lambda_{\zeta,i}, \lambda_{T,i}, F_{\text{dis},i} \quad (41a)$$

$$\underline{v} \leq v_i \leq \bar{v}, \quad (41b)$$

$$\underline{v}^2 \leq z_i \leq \bar{v}^2, \quad (41c)$$

$$\underline{\zeta} \leq \zeta_i \leq \bar{\zeta}, \quad (41d)$$

$$0 \leq T_{\text{batt},i} \leq \bar{T}_{\text{batt}}, \quad (41e)$$

$$\underline{F_{\text{m}}} \leq F_{\text{m},i} \leq \bar{F_{\text{m}}}, \quad (41f)$$

$$\underline{F_{\text{brk}}} \leq F_{\text{brk},i} \leq \bar{F_{\text{brk}}} \quad (41g)$$

and the more elaborate

$$\underline{P_{\text{m}}} \lambda_{v,i} \leq F_{\text{m},i} \leq \bar{P_{\text{m}}} \lambda_{v,i}, \quad (42a)$$

$$\underline{P_{\text{batt}}} \lambda_{v,i} \leq F_{\text{batt},i} \leq \bar{P_{\text{batt}}} \lambda_{v,i}, \quad (42b)$$

$$\underline{P_{\text{fc}}} \lambda_{v,i} \leq F_{\text{fc},i} \leq \bar{P_{\text{fc}}} \lambda_{v,i}. \quad (42c)$$

Lastly, are the list of relaxed convex inequalities

$$1 \leq v_i \lambda_{v,i}, \quad (43a)$$

$$v_i^2 \leq z_i, \quad (43b)$$

$$q_{\text{m}}(F_{\text{m},i}, z_i) + P_{\text{aux},i} \lambda_{v,i} \leq F_{\text{fc},i} + F_{\text{batt},i}, \quad (43c)$$

$$\alpha F_{\text{batt},i}^2 \Delta_{\text{s},i} \leq \lambda_{\zeta,i} \lambda_{v,i}, \quad (43d)$$

$$\lambda_{T,i} \leq h T_{\text{batt},i} \lambda_{v,i}, \quad (43e)$$

$$F_{\text{chr},i} \leq F_{\text{batt},i}, \quad (43f)$$

$$F_{\text{batt},i} \leq F_{\text{dis},i}. \quad (43g)$$

The constraint (43a) implies that v is strictly positive and thus z as well due to (43b). Nevertheless, in order

to emulate being stationary at station stops in (40), z_{stop} is set to a small positive value that approaches zero. During station stops $F_{\text{ext},j}$ is zeroed in order to successfully emulate a stationary state with brakes locked (see (2)). Since the optimized speed profile is strictly positive, the sampling intervals during station stops $\Delta_{\text{s},j}$ are adjusted *a priori* to the multiplication of dwell (wait) time by $\sqrt{z_{\text{stop}}}$. Although the optimized speed at station stops never attains zero, in practice, it can be zeroed without affecting feasibility or optimality if z_{stop} was small enough.

In order to prove the optimality of the proposed formulation, all relaxed constraints (43) need to be proven to hold with equality. The following justifies inequality tightness:

- (43a): the summation $\sum_i \lambda_{v,i}$ is fixed through (39) and v has the incentive to drop due to losses in (3);
- (43b): z has incentive to drop due to penalty (37) but v is constrained from beneath by (43a);
- (43c): F_{batt} has incentive to go negative to gather free charge and minimize F_{fc} while q_{m} has incentive to move the train to fulfill journey time (39);
- (43d): the original expression (17) when relaxed, $\Delta_\zeta \geq (\alpha F_{\text{batt}}^2 v^2 + \beta F_{\text{batt}} v) \Delta_{\text{t}}$, would rather have positive F_{batt} to move the train and push Δ_ζ to zero or negative to gain free charge;
- (43e),(43f),(43g): if the upper temperature bound in (41e) is reached, (36) would rather tighten (43e), (43f), and (43g), before relying on the active cooling system command F_{act} that is penalized in (37).

The optimization problem proposed above is convex because it penalizes a convex quadratic cost function subject to linear equality and convex inequality constraints. It can be formulated and solved as a second-order cone program.

5. CONCLUSION

Models for the the concurrent optimization of hybrid train speed, EMS, and battery thermals, were presented. A relaxed convex problem was formulated in order to alleviate computational concerns while the tightness of the relaxed constraints was justified. The accuracy of the proposed convex models was proven by graphical means and analyzing the convexity properties of the original first-principle models. The benefit from this holistic optimization approach is yet to be verified on a real case study, after which optimizing fuel cell thermals and optimizing the operation of singular fuel cell stacks independently is to be investigated.

REFERENCES

- Boyd, S. and Vandenberghe, L. (2004). *Convex optimization*. Cambridge University Press.
- Chen, B., Evangelou, S.A., and Lot, R. (2019). Series hybrid electric vehicle simultaneous energy management and driving speed optimization. *IEEE/ASME Transactions on Mechatronics*, 24(6), 2756–2767. doi:10.1109/tmech.2019.2943320.
- De Almeida, A.T., Ferreira, F.J.T.E., and Fong, J.A.C. (2011). Standards for efficiency of electric motors. *IEEE Industry Applications Magazine*, 17(1), 12–19. doi:10.1109/mias.2010.939427.
- Douglas, H., Weston, P., Kirkwood, D., Hillmanssen, S., and Roberts, C. (2016). Method for validating the

- train motion equations used for passenger rail vehicle simulation. *Proceedings of the Institution of Mechanical Engineers, Part F: Journal of Rail and Rapid Transit*, 231(4), 455–469. doi:10.1177/0954409716631784.
- Ebbesen, S., Elbert, P., and Guzzella, L. (2012). Battery state-of-health perceptive energy management for hybrid electric vehicles. *IEEE Transactions on Vehicular Technology*, 61(7), 2893–2900. doi:10.1109/tvt.2012.2203836.
- Ebbesen, S., Salazar, M., Elbert, P., Bussi, C., and Onder, C.H. (2018). Time-optimal control strategies for a hybrid electric race car. *IEEE Transactions on Control Systems Technology*, 26(1), 233–247. doi:10.1109/tcst.2017.2661824.
- Filippi, A.D., Stockar, S., Onori, S., Canova, M., and Guezennec, Y. (2010). Model-based life estimation of li-ion batteries in phevs using large scale vehicle simulations: An introductory study. In *2010 IEEE Vehicle Power and Propulsion Conference*. IEEE.
- García, P., Torreglosa, J.P., Fernández, L.M., and Jurado, F. (2013). Control strategies for high-power electric vehicles powered by hydrogen fuel cell, battery and supercapacitor. *Expert Systems with Applications*, 40(12), 4791–4804. doi:10.1016/j.eswa.2013.02.028.
- Ghaviha, N., Bohlin, M., Holmberg, C., and Dahlquist, E. (2019). Speed profile optimization of catenary-free electric trains with lithium-ion batteries. *Journal of Modern Transportation*, 27(3), 153–168. doi:10.1007/s40534-018-0181-y.
- Jia, Y., Jibrin, R., and Gorges, D. (2020). Energy-optimal adaptive cruise control for electric vehicles based on linear and nonlinear model predictive control. *IEEE Transactions on Vehicular Technology*, 69(12), 14173–14187. doi:10.1109/tvt.2020.3044265.
- Jibrin, R., Hillmanssen, S., Roberts, C., Zhao, N., and Tian, Z. (unpublished). Convex optimization of speed and energy management system for fuel cell hybrid trains. In *2021 IEEE Vehicle Power and Propulsion Conference (VPPC), October 25-28*. URL <https://arxiv.org/abs/2109.13833>.
- Kim, J., Park, Y., Fox, J.D., Boyd, S., and Dally, W. (2020). Optimal operation of a plug-in hybrid vehicle with battery thermal and degradation model. In *2020 American Control Conference*.
- Lhomme, W., Letrouvé, T., Boulon, L., Jemeï, S., Bouscayrol, A., Chauvet, F., and Tournez, F. (2018). IEEE VTS motor vehicles challenge 2019 – energy management of a dual-mode locomotive. In *2018 IEEE Vehicle Power and Propulsion Conference (VPPC)*. IEEE.
- Li, G., Zhuang, W., Yin, G., Ren, Y., and Ding, Y. (2019). Energy management strategy and size optimization of a lfp/lto hybrid battery system for electric vehicle. *SAE Technical Paper Series*. doi:10.4271/2019-01-1003.
- Lin, J., Liu, X., Li, S., Zhang, C., and Yang, S. (2021). A review on recent progress, challenges and perspective of battery thermal management system. *International Journal of Heat and Mass Transfer*, 167. doi:10.1016/j.ijheatmasstransfer.2020.120834.
- Lucu, M., Martinez-Laserna, E., Gandiaga, I., Liu, K., Camblong, H., Widanage, W.D., and Marco, J. (2020). Data-driven nonparametric li-ion battery ageing model aiming at learning from real operation data - part b: Cycling operation. *Journal of Energy Storage*, 30. doi:10.1016/j.est.2020.101410.
- Moura, S.J., Stein, J.L., and Fathy, H.K. (2013). Battery-health conscious power management in plug-in hybrid electric vehicles via electrochemical modeling and stochastic control. *IEEE Transactions on Control Systems Technology*, 21(3), 679–694. doi:10.1109/tcst.2012.2189773.
- Pagenkopf, J. and Kaimer, S. (2014). Potentials of alternative propulsion systems for railway vehicles – a techno-economic evaluation. In *2014 Ninth international conference on ecological vehicles and renewable energies (EVER)*. IEEE.
- Park, S. and Ahn, C. (2021). Model predictive control with stochastically approximated cost-to-go for battery cooling system of electric vehicles. *IEEE Transactions on Vehicular Technology*, 70(5), 4312–4323. doi:10.1109/tvt.2021.3073126.
- Pelletier, S., Jabali, O., Laporte, G., and Veneroni, M. (2017). Battery degradation and behaviour for electric vehicles: Review and numerical analyses of several models. *Transportation Research Part B: Methodological*, 103, 158–187. doi:10.1016/j.trb.2017.01.020.
- Scheepmaker, G.M., Goverde, R.M.P., and Kroon, L.G. (2017). Review of energy-efficient train control and timetabling. *European Journal of Operational Research*, 257(2), 355–376. doi:10.1016/j.ejor.2016.09.044.
- Stroe, A.I. (2018). *Analysis of Performance and Degradation for Lithium Titanate Oxide Batteries*. Thesis. doi:10.5278/VBN.PHD.ENG.00039.
- Tang, L. (2017). *Optimal energy management strategy for hybrid electric vehicles with consideration of battery life*. Thesis.
- Thorstensen, B. (2000). A parametric study of fuel cell system efficiency under full and part load operation. *Journal of Power Sources*, 92, 9–16.
- Wang, J., Liu, P., Hicks-Garner, J., Sherman, E., Soukiazian, S., Verbrugge, M., Tatara, H., Musser, J., and Finamore, P. (2011). Cycle-life model for graphite-lifepo4 cells. *Journal of Power Sources*, 196(8), 3942–3948. doi:10.1016/j.jpowsour.2010.11.134.
- Wipke, K.B., Cuddy, M.R., and Burch, S.D. (1999). Advisor 2.1: A user-friendly advanced powertrain simulation using a combined backward/forward approach. *IEEE Transactions on Vehicular Technology*, 48(6).
- Wu, C., Xu, B., Lu, S., Xue, F., Jiang, L., and Chen, M. (2021). Adaptive eco-driving strategy and feasibility analysis for electric trains with on-board energy storage devices. *IEEE Transactions on Transportation Electrification*, 1–1. doi:10.1109/tte.2021.3050470.
- Xiao, Z., Chen, H., Guo, J., Wang, Q., Sun, P., and Feng, X. (2021). Joint optimization of speed and voltage trajectories for hybrid electric trams. *IEEE Transactions on Industry Applications*, 1–1. doi:10.1109/tia.2021.3102881.
- Yue, M., Jemei, S., Gouriveau, R., and Zerhouni, N. (2019). Review on health-conscious energy management strategies for fuel cell hybrid electric vehicles: Degradation models and strategies. *International Journal of Hydrogen Energy*, 44(13), 6844–6861. doi:10.1016/j.ijhydene.2019.01.190.